Journal of Environment and Sustainable Mining

Effect of Bubble-Particle Interactions on Collection Efficiency of Froth Flotation

Behzad Shahbazi [1*]
[1] Mining Engineering Department, Tarbiat Modares University, Tehran, Iran.

ARTICLE INFO

Article type:
Research Article

Article history:
Received: 2025-04-10
Received in revised form: 2025-05-23
Accepted: 2025-06-22
Available online: 2025-06-29

Keywords:
Flotation,
Rate Constant,
Collision,
Attachment,
Detachment.

ABSTRACT

Bubble-particle interactions have a great effect on the efficiency of particle collection in froth flotation, and by using them, the flotation rate constant (k) can be increased. In this research, the relationship between k and bubble surface area flux (Sb) was investigated using bubble-particle interactions. Bubble-particle collision, attachment, and detachment efficiencies were calculated under different flow regimes. The flotation rate increased with the increase of both the collision and attachment efficiencies. Maximum Stokes collision efficiency was obtained as 81.57% with the Sb of 27.43 1/s, particle size of -500+420 µm, and k of 0.97 1/min. Maximum Stokes attachment efficiency was obtained as 55.9% with a particle size of -37 µm, Sb of 34.2 1/s, and k of 1.65 1/min. Maximum detachment efficiency was obtained as 98.54% with the particle size of -500+420 µm, Sb of 12.16 1/s, and k of 0.44 1/min. So, Bubble-particle collection efficiency was increased with the increase of the Sb. Thus, an increase in k can be attributed to an increase in both the collision and attachment efficiencies due to an increase in the S_b.

Cite this article: Shahbazi, B. (2025). Effect of Bubble-Particle Interactions on Collection Efficiency of Froth Flotation. *Journal of Environment and Sustainable Mining*, 1(2), 11-21. https//doi.org/10.22111/jesm.2024.47721.1013

Publisher: University of Sistan and Baluchestan.
DOI: https//doi.org/10.22111/jesm.2024.47721.1013

* Corresponding author: **Behzad Shahbazi**
E-mail address: bzshahbazi@yahoo.com

1. Introduction

Froth flotation has been arguably the most important method of mineral beneficiation over the past 100 years and is likely to remain so well into the future. Many researchers investigated the surface area flux [1-12], and in some cases, researchers have focused on the effect of bubble surface area flux (S_b), on the flotation rate [9-12]. Gorain et al. investigated the effect of gas dispersion properties on the flotation rate constant, k, in plant and pilot scale mechanical cells over a range of operating conditions for four impeller types. They found that the flotation rate constant was not readily related to the bubble size, gas holdup, or superficial gas velocity individually, but it was related to the S_b. For example, for shallow froths, the relationship was linear. It has also been found that S_b was strongly related to the k and that the relationship was linear, as represented by the following equations [7,8]:

$$k = \alpha R_f S_b \tag{1}$$

$$S_b = 6J_g / d_{32} \tag{2}$$

Where, J_g is the superficial gas velocity, d_{32} is the Sauter mean diameter of the bubble, α is the "floatability factor", which encompasses the contribution of particle size and hydrophobicity [13], and R_f is the froth recovery factor, which is defined as the ratio of the overall flotation rate constant and the collection zone rate constant [8].

Understanding the various micro processes involved in the collection of solid particles by air bubbles, namely collision, attachment, and detachment, is a fundamental step toward predicting the k [14-17]. The efficiency of adhesion determines the selectivity of a flotation process, while its recovery depends critically on the collision efficiency. Also, some of the particles are detached from the surface due to the inertia force and turbulence in a flotation cell.

In this research, a theoretical analysis of the flotation rate was conducted based on the bubble-particle collision, attachment, and detachment efficiencies. Also, the effect of S_b and particle size on the k of quartz particles was studied. According to author's knowledge, for the first time, the relationship between k and S_b was studied using bubble-particle interactions and, consequently, has important implications regarding the optimization, scale-up, and design of mechanical flotation cells.

Also, so far, researchers have developed different models to determine the efficiency of collecting particles smaller than 100 μm (the usual particle size in the flotation process) in flotation and have experimentally investigated their models. However, not much research has been done on coarse particles (larger than 100 μm) that have high collision and detachment efficiency. In this research, the flotation rate of coarse particles (up to 500 μm) is determined, and for the first time, according to the author knowledge, an attempt is made to interpret the low flotation rate of coarse particles using the low efficiency of collecting coarse particles. These results will help researchers to better understand the micro-processes of flotation, such as collision, attachment, and detachment efficiency. Therefore, this research can be useful in the development of coarse particle flotation methods.

2. Materials and methods

Flotation experiments were carried out in a mechanical laboratory flotation cell. An impeller diameter of 0.07 m was used for pulp agitation, and a cell with a square section was used in which the length and height were 0.13 and 0.12 m, respectively. The impeller rotating speed was 900, 1000, 1100, and 1200 rpm, and the air flow rate was 60, 120, 180, and 240 l/h. Quartz particles of eight size classes containing -37, -53+37, -75+53, -106+75, -212+106, -300+212, -420+300 and -500+420 μm were used for flotation experiments. The frother was MIBC (methyl iso-butyl carbinol) with a concentration of 22.4 ppm. The flotation experiments were carried out by dodecyl amine collector (50 g/t) at the natural pH of 8.5 using local tap water. When the S_b values were set, all the size fractions were floated together under those exact

conditions (Table 1). $k = \alpha R_f S_b$ is not universally accepted and certainly can only be valid up to a certain S_b (a limit on the S_b before the cell boils). So, in this investigation, S_b was 10.21 to 34.2 1/s. Also, in all the experiments, the froth depth was shallow and the froth recovery factor (R_f) was assumed to be equal to 1.

Table 1. Flotation tests conditions.

Gas Flow Rate (l/h)	**60**	**60**	**60**	**60**	**120**	**120**	**120**	**120**	**180**	**180**	**180**	**180**	**240**	**240**	**240**	**240**
Impeller Speed (rpm)	**900**	**1000**	**1100**	**1200**	**900**	**1000**	**1100**	**1200**	**900**	**1000**	**1100**	**1200**	**900**	**1000**	**1100**	**1200**
d_b (μm)	830	750	690	630	830	750	680	620	820	750	680	620	820	750	680	620
ε_g (%)	2.86	3.75	4.75	5.87	3.62	4.71	5.93	7.30	4.08	5.29	6.65	8.17	4.48	5.79	7.27	8.92
J_g (cm/s)	0.1	0.1	0.1	0.1	0.2	0.2	0.2	0.2	0.3	0.3	0.3	0.3	0.4	0.4	0.4	0.4
S_b (1/s)	10.21	10.88	11.53	12.16	16.77	17.94	19.08	20.19	22.69	24.31	25.89	27.43	28.23	30.28	32.27	34.2
Re_b	307	229	174	133	303	226	171	131	301	224	170	130	299	223	169	130
ε (W/kg)	2.15	2.95	4.18	5.98	2.15	2.95	4.18	5.98	2.15	2.95	4.18	5.98	2.15	2.95	4.18	5.98

The air flow rate and the impeller speed were set, and the float product was collected at the time intervals of 1, 2, 3, and 5 minutes. The recovery, R, was determined as a function of time, t, and k was calculated. The batch-wise flotation of mineral particles may be described by a first-order rate equation where the removal rate of particles is given by:

$$\frac{dC}{dt} = -kC \tag{3}$$

Where C is the particle concentration in mass per unit volume. The k was calculated assuming the first-order rate equation for a batch cell, $R = R^*(1 - \exp(-kt))$, and plotting $\ln(1 - R/R^*)$ versus t. Where R^* is the recovery in infinite time.

The bubble size distribution was measured in a device similar to McGill's bubble viewer [18]. It consisted of a sampling tube attached to a viewing chamber with a window inclined 15 degrees from vertical. The closed assembly was filled with water of a similar nature to that in the flotation cell (to limit changes in the bubble environment during the sampling). Then the tube was immersed in the desired location below the froth. Bubbles rose into the viewing chamber and were imaged by a digital camera as they slid up the inclined window, which was illuminated from behind [18]. In this research, at first, frother and collector (because amines may act as a frother) were added to the water of the cell, and then the viewing chamber was filled with water from the cell to prevent bubble coalescence.

The Washburn method was used to measure the contact angle on the powder. The contact angle of quartz particles was measured using a Lauda tensiometer (TE3) after flotation tests. The Lauda tensiometer simplifies the characterization of the wetting behavior of the whole surface. The contact angle was measured by means of the precise adjustment of the immersion/receding rate and micrometer-accurate measurement

of the immersion dept. Contact angle of the quartz sample was obtained as 89.7 degrees using Lauda tensiometer (TE3).
Superficial gas velocity was calculated using the air flow rate and the area cross-section of the cell, with consideration of the area occupied by the impeller shaft. The input power was inferred from the electrical measurements and measuring the entrance amperage and voltage to the electrical motor of the flotation equipment.
The following flowchart shows all the calculation steps and specifies the methods of using the experimental data in each model (Fig. 1).

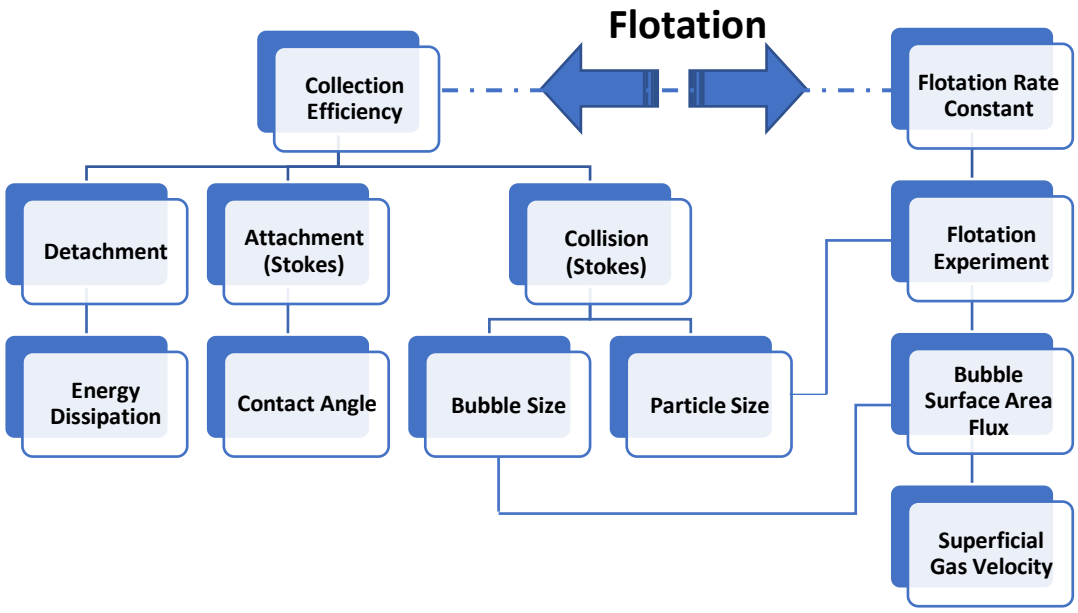

Fig. 1. Calculation and laboratory steps in conducting the research.

3. Theory

The k is proportional to the collection efficiency [19]. This equation can be seen as the form of equation below [20]:

$$E_{col} = E_c E_a (1 - E_d) \quad (4)$$

Where, E_c is the bubble-particle collision efficiency, E_a is the bubble-particle attachment efficiency and E_d is bubble-particle detachment efficiency. Equations of the bubble-particle collision, attachment, and detachment efficiencies under different flow conditions are given in Table 2.

Table 2. Equations for calculating collision, attachment and detachment efficiencies.

Bubble-particle Interaction	Flow Conditions	Equation		
Collision Efficiency [27, 28]	Flint-Howarth	$E_{c-FH} = \frac{v_p}{v_p + v_b}$	Stokes	$E_{c-St} = \frac{3}{2}(d_p/d_b)^2$
	Potential	$E_{c-P} = 3d_p/d_b$	Intermediate	$E_{c-I} = (d_p/d_b)^2\left[\frac{3}{2} + \frac{4\,Re_b^{0.72}}{15}\right]$
Attachment Efficiency [28, 29]	Yoon	$E_{a-Y} = \sin^2\left[2\arctan\exp\left(\frac{-(45+8Re_b^{0.72})v_b t_i}{15d_b(d_b/d_p+1)}\right)\right]$		
	Stokes	$E_{a-St} = \operatorname{sech}^2\left(\frac{2v_p A_{St} t_i}{d_p + d_b}\right)$, $A_{St} = \frac{v_b}{v_p} + 1 - \frac{3}{4}\left(1+\frac{d_p}{d_b}\right)^{-1} - \frac{1}{4}\left(1+\frac{d_p}{d_b}\right)^{-3}$		
	Potential	$E_{a-P} = \operatorname{sech}^2\left(\frac{2v_p A_P t_i}{d_p + d_b}\right)$, $A_P = \frac{v_b}{v_p} + 1 + \frac{1}{2}\left(1+\frac{d_p}{d_b}\right)^{-3}$		
Detachment Efficiency [30]	Bloom and Heindel	$E_d = \exp\left[0.5\left(1-\frac{1}{Bo^*}\right)\right]$, $Bo^* = \frac{d_p^2\left[\Delta\rho_s g + 1.9\rho_s \varepsilon^{\frac{2}{3}}\left(\frac{d_p}{2}+\frac{d_b}{2}\right)^{-\frac{1}{3}}\right]}{6\sigma\sin\left(\pi-\frac{\theta}{2}\right)\sin\left(\pi+\frac{\theta}{2}\right)}$ $+ \frac{1.5d_p\left(\frac{4\sigma}{d_b} - d_b\rho g\right)\sin^2\left(\pi-\frac{\theta}{2}\right)}{6\sigma\sin\left(\pi-\frac{\theta}{2}\right)\sin\left(\pi+\frac{\theta}{2}\right)}$		
Detachment Frequency [31]	Mika and Fuerstenau	$Z' = \sqrt{C_1}\varepsilon^{\frac{1}{3}}(d_p+d_b)^{\frac{-2}{3}}$, $1.61 \le C_1 \le 2.33$		

v_p : particle velocity, v_b : bubble velocity, d_p : particle diameter, d_b : bubble diameter, t_i : induction time, Re_b : bubble Reynolds number, Bo^* : Bond number, ε : energy dissipation, C_1 : empirical value, θ : contact angle, g: acceleration due to gravity, σ : surface tension, ρ_s : particle density, $\Delta\rho_s = (\rho_s - \rho)$, ρ : fluid density

The five parameters of d_{32}, v_b, v_p, Re_b and t_i are necessary parameters for calculating the collision, attachment, and detachment efficiencies that the parameters are obtained using the following equations (Eq. 5-9). The mean bubble diameter adopted was the Sauter diameter, calculated by the equation below [21]:

$$d_{32} = \frac{\sum n_i d_i^3}{\sum n_i d_i^2} \tag{5}$$

Where, n is the number of bubbles and d is the bubble diameter. If the surface of a drop or bubble is immobile for any reason, the floating velocity is the same as that of a solid sphere and the bubble raise velocity can be described by the Stokes equation [22]:

$$v_b = \frac{d_b^2}{18\nu} g \quad (6)$$

Where ν is the kinematic viscosity. Also, particle settling velocity can be described by the following equation [10]:

$$v_p = \sqrt{\frac{3g(\rho_s - \rho)d_p}{\rho}} \quad (7)$$

Where neither Newton's nor Stokes' laws apply; rather, there is another equation for calculating the particle settling velocity as follows [23]:

$$V_p = \frac{20.52\eta}{d_p \rho}\left(\left[1 + 0.0921\left(\frac{d_p^3(\rho_s - \rho)\rho g}{0.75\eta^2}\right)^{0.5}\right]^{0.5} - 1\right)^2 \quad (8)$$

Where η is the dynamic viscosity. The bubble Reynolds number is another effective hydrodynamic parameter on the k, which is calculated by the equation below [24]:

$$Re_b = v_b d_b \rho / \eta \quad (9)$$

The induction time is a function of the particle size and contact angle, which can be determined by the equation below [25, 26]:

$$t_i = \frac{75}{\theta} d_p^{0.6} \quad (10)$$

4. Results and discussion

The effect of S_b on flotation rate of quartz particles is given in Fig. 2. The Flotation rate was increased with the increase of the S_b and a decrease in the particle size. The maximum k was obtained as 1.89 1/min, when the particle size, impeller speed, and S_b were -37 µm, 1100 rpm, and 32.27 1/s, respectively. Furthermore, the minimum k was obtained as 0.32 1/min for the particle size of -500+420 µm, the impeller speed of 1100 rpm, and the S_b of 11.53 1/s.

4.1. The effect of bubble-particle collision efficiency on the k

Bubble-particle collision efficiency was calculated under different flow regimes, and the following results were obtained. With the increase in the particle size and S_b, the bubble-particle collision efficiency was increased as well. So, an increase in k can be due to an increase in the collision efficiency.

According to Fig. 3, the Flint-Howarth collision efficiency was calculated for different particle sizes ($0.19 < E_{c-FH} < 41.51\%$). The maximum Flint-Howarth collision efficiency was obtained as 41.51% with the k of 0.97 1/min, S_b of 27.43 1/s and particle size of -500+420 µm. The Flint-Howarth collision efficiency for coarse particles was much lower than that of other models. So perhaps this model is not applicable to coarse particles.

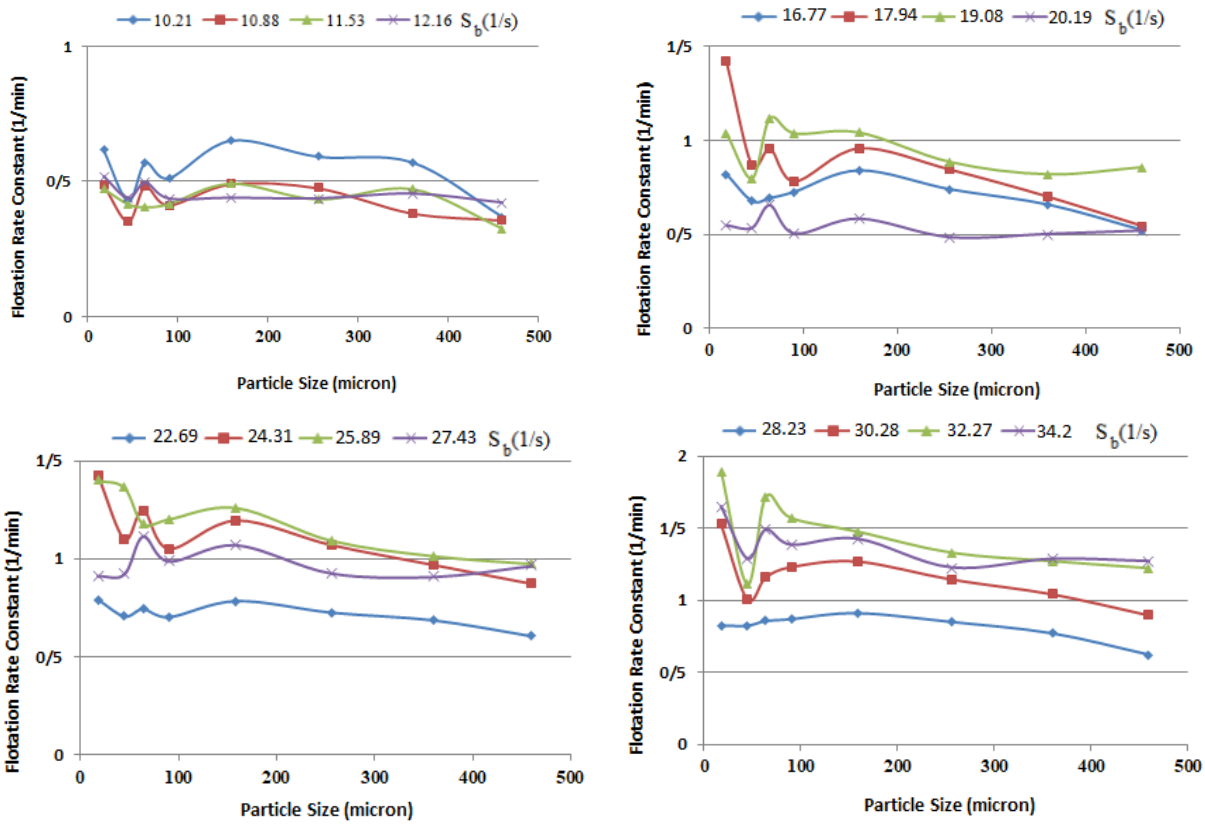

Fig. 2. The effect of on the flotation rate of quartz particles.

According to Fig. 3, the Stokes collision efficiency was calculated for the different S_b and particle sizes ($0.07 < E_{c-S} < 81.57\%$). The maximum Stokes collision efficiency was obtained as 81.57% with the S_b of 27.43 1/s, particle size of -500+420 µm and k of 0.97 1/min. The minimum collision efficiency was obtained as 0.07% with the particle size of -37 µm and S_b of 10.21 1/min. This model appears to give a good estimation for bubble-particle collision efficiency of both the coarse and fine particle sizes.
Also, the collision efficiency was calculated according to the Potential and Intermediate flow conditions (Fig. 3). The Potential and Intermediate collision efficiencies were exaggerated as the collision efficiency of coarse particles (-300+212, -420+300, and -500+420 µm) was more than 100%. So, these models were not applicable to coarse particles.

4.2. The effect of bubble-particle attachment efficiency on the k

The effect of S_b and particle size on the bubble-particle attachment efficiency is shown in Fig. 3. Both the k and attachment efficiency were increased with the increase of the S_b. Also, the attachment efficiency was decreased with increasing of the particle size. So, increasing the k, due to the increase in the S_b, can be attributed to an increase in the attachment efficiency.

The maximum Yoon's, Stokes', and Potential's attachment efficiencies were obtained as 94.8, 55.9, and 15.5%, respectively. The maximum attachment efficiency was obtained with the particle size of -37 µm, S_b of 34.2 1/s and k of 1.65 1/min. The Yoon's attachment efficiency was more than the other attachment efficiencies, and the potential attachment efficiency was much lower than that of both the Yoon's and Stokes' attachment efficiencies.

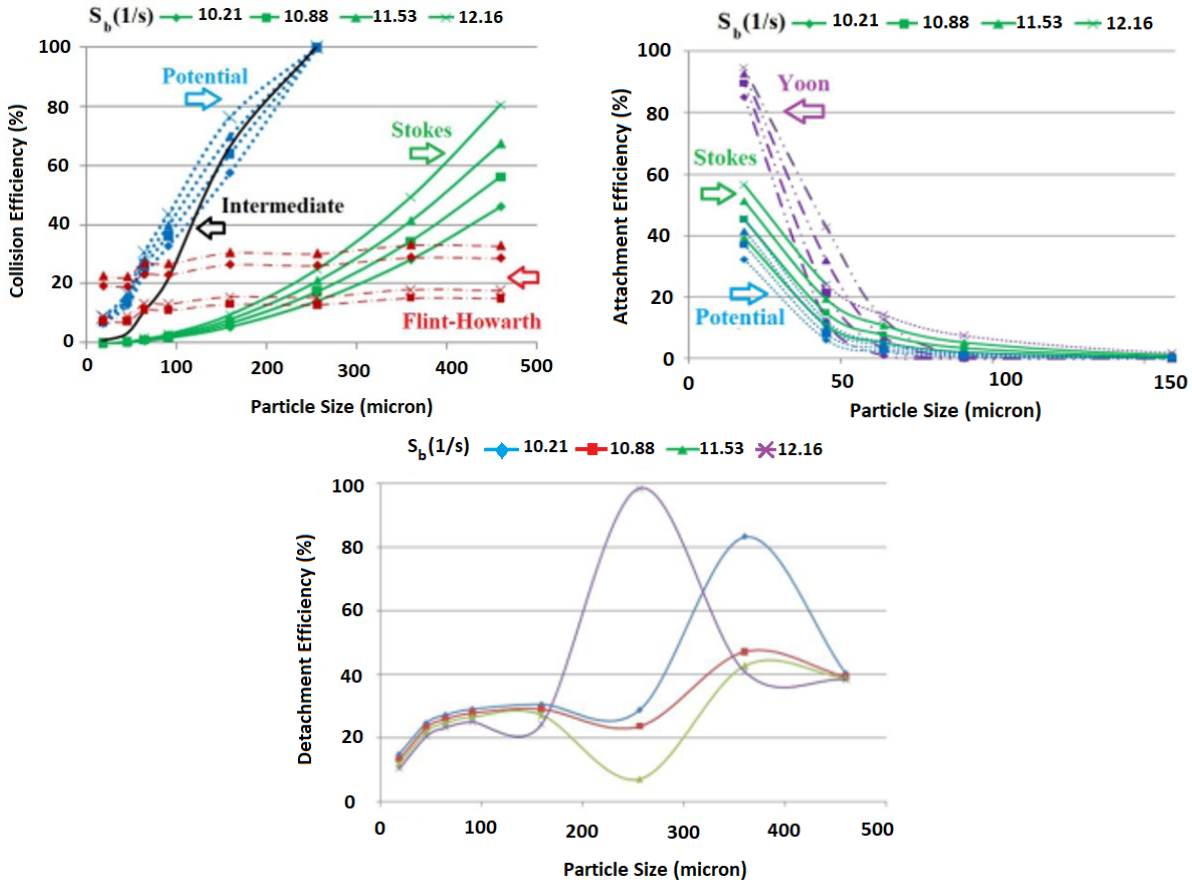

Fig. 3. The effect of particle size on the bubble-particle collision, attachment and detachment efficiencies.

4.3. The effect of bubble-particle detachment efficiency on the k

In this research, detachment frequency was in the range of 160-360 1/s. The maximum detachment frequency obtained was 360 1/s with the energy dissipation of 5.98 W/kg and bubble-particle aggregate diameter, $d_b + d_p$, of 0.64 mm. The minimum detachment frequency obtained was 160 1/s with the energy dissipation of 2.15 W/kg and bubble-particle aggregate diameter of 1.3 mm. So, detachment frequency increased with the increase in the energy dissipation and the decrease in the bubble-particle aggregate diameter. The k increased with a decrease in the detachment frequency.

Detachment efficiency increased with increasing of the particle size. According to Fig. 3, the maximum detachment efficiency obtained was 98.54% with the S_b of 12.16 1/s, particle size of -500+420 µm and k of 0.44 1/min. Also, the minimum detachment efficiency obtained was 4.56% for the particle size of -300+212 µm, S_b of 32.27 1/s and k of 1.33 1/min.

4.4. Efficiency of collecting particles with the bubbles

The effect of S_b and particle size on the bubble-particle collection efficiency is shown in Fig. 4. Since the bubble-particle collision, attachment, and detachment efficiencies have already been calculated, calculating the bubble-particle collection efficiency is now possible. The results showed that bubble-particle collection efficiency was increased with the increase in the S_b. Difficulty in floating fine particles is attributed to the low efficiency of bubble-particle collision efficiency while difficulty in floating coarse particles is due to the high efficiency of bubble-particle detachment. According to Fig. 3, the bubble-

particle collection efficiency of both the fine and coarse particles was low. So, the maximum bubble-particle collection efficiency was obtained for the medium size classes of the -53+37, -75+53, -106+75, and -212+106 µm.

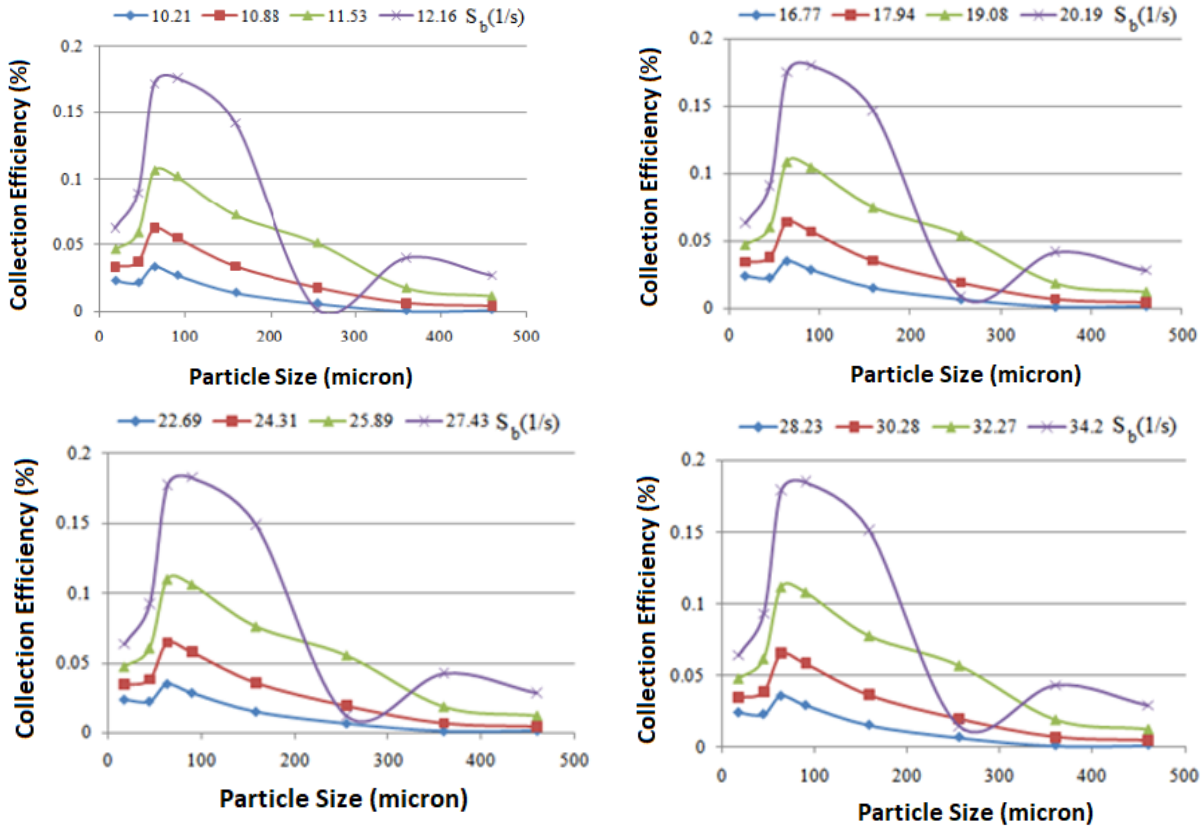

Fig. 4. The effect of S_b and particle size on the bubble-particle collection efficiency.

5. Conclusion

In this research, the effect of S_b and particle size on the flotation rate of quartz particles was investigated, and the following conclusions were made:

- The maximum k was obtained as 1.89 1/min, when the particle size, impeller speed, and $S_b$were -37 µm, 1100 rpm, and 32.27 1/s, respectively. Furthermore, the minimum k was obtained as 0.32 1/min for the particle size of -500+420 µm, the impeller speed of 1100 rpm, and the S_b of 11.53 1/s. So, the flotation rate increased with the increase in the S_b and a decrease in the particle size.
- Stokes collision efficiency was calculated for different S_b and particle sizes. The maximum Stokes collision efficiency was obtained as 81.57% with the S_b of 27.43 1/s, particle size of -500+420 µm and k of 0.97 1/min. So, an increase in k can be due to an increase in the S_b and thus collision efficiency.
- The maximum Stokes attachment efficiency was obtained 55.9% with the particle size of -37 µm, S_b of 34.2 1/s and k of 1.65 1/min. So, an increase in k can be attributed to an increase in attachment efficiency.
- Detachment efficiency increased with increasing of the particle size. The maximum detachment efficiency obtained was 98.54% with the S_b of 12.16 1/s, particle size of -500+420 µm and k of 0.44 1/min.

- Bubble-particle collection efficiency was increased with the increase in the S_b. Thus, an increase in k can be attributed to an increase in both the collision and attachment efficiencies due to an increase in the S_b.

Ethical Considerations
The authors avoided data fabrication, falsification, and plagiarism, and any form of misconduct.

Funding
This research did not receive any specific grant from funding agencies in the public, commercial, or not-for-profit sectors.

Conflict of Interest
The authors declare no conflict of interest.

References

[1] Anzoom, S. J., Ghislain, B., Ata, S. (2023). Coarse particle flotation: A review. *Minerals Engineering*, 206. https://doi.org/10.1016/j.mineng.2023.108499
[2] Shahbazi B., Samadian H., (2023), Computational Modelling of Gas Dispersion Parameters in Froth Flotation, 4th international conference on chemistry and chemical engineering, Tehran, Iran.
[3] Gomez, C.O., Maldonado, M. (2022). Modelling Bubble Flow Hydrodynamics: Drift-Flux and Molerus Models, *Minerals*, (12)12 :1502. https://doi.org/10.3390/min12121502
[4] Asgari, K., Huang, Q., Khoshdast, H., Hassanzadeh, A. (2022). A Review on Bio flotation of Coal and Minerals: Classification, Mechanisms, Challenges, and Future Perspectives. *Mineral Processing and Extractive Metallurgy Review*, (45)1: 46-76. https://doi.org/10.1080/08827508.2022.2121919
[5] Sarhan, A. R. J. & Brooks N. G. (2018), CFD model simulation of bubble surface area flux in flotation column reactor in presence of minerals. *International Journal of Mining Science and Technology*, (28) 6: 999-1007. https://doi.org/10.1016/j.ijmst.2018.05.004
[6] Gorain, B. K., Franzidis, J. P. & Manlapig, E. V. (1995). Studies on impeller type, impeller speed and air flow rate in an industrial scale flotation cell. Part 1: Effect on bubble size distribution, *Minerals Engineering*, 8(6): 615-635. https://doi.org/10.1016/0892-6875(95)00025-L
[7] Gorain, B. K., Franzidis, J. P. & Manlapig, E. V., (1995). Studies on impeller type, impeller speed and air flow rate in an industrial scale flotation cell. Part 2: Effect on gas holdup. *Minerals Engineering*, 8: 1557-1570. https://doi.org/10.1016/0892-6875(95)00118-2
[8] Gorain, B. K., Franzidis, J. P. & Manlapig, E. V., (1996). Studies on impeller type, impeller speed and air flow rate in an industrial scale flotation cell. Part 3: Effect on superficial gas velocity. *Minerals Engineering*, 9(6): 639-654. https://doi.org/10.1016/0892-6875(96)00052-0
[9] Leiva, J., Vinnett, L., Contreras, F. & Yianatos, J., (2010). Estimation of the actual bubble surface area flux in flotation. *Minerals Engineering*, 23: 888–894. https://doi.org/10.1016/j.mineng.2010.01.013
[10] Massinaei, M. & Doostmohammadi, R., (2010). Modeling of bubble surface area flux in an industrial rougher column using artificial neural network and statistical techniques. *Minerals Engineering*, 23(2): 83–90. https://doi.org/10.1016/j.mineng.2009.10.005
[11] Pérez-Garibay, R., Estrada-Ruiz, R. H. & Gallegos-Acevedo, P. M., (2010). Relationship between the bubble surface flux that overflows and the mass flow rate of solids in the concentrate of flotation processes. *Minerals Engineering*, 23(7): 541-548. https://doi.org/10.1016/j.mineng.2009.12.008
[12] Pérez-Garibay, R., Martínez-Ramos, E. & Rubio, J., (2012). Gas dispersion measurements in microbubble flotation systems. *Minerals Engineering*, 26: 34-40. https://doi.org/10.1016/j.mineng.2011.10.006
[13] Hernandez-Aguilar, J. R., Rao, S. R. & Finch, J. A., (2005). Testing the k-Sb relationship at the

microscale. *Minerals Engineering*, 18(6): 591-598. https://doi.org/10.1016/j.mineng.2004.10.003
[14] Nazari, S., Shafaei, S.Z., Gharabaghi, M., Ahmadi, R., Shahbazi, B., Tehranchi, A. (2020). New approach to quartz coarse particles flotation using nanobubbles, with emphasis on the bubble size distribution. *International Journal of Nanoscience*, 19(01): 1850048. https://doi.org/10.1142/S0219581X18500485
[15] Parkes, S., Wang, P., Galvin, K.P. (2022). Investigating the System Flotation Kinetics of Fine Chalcopyrite in a REFLUX™ Flotation Cell using a Standardized Flotation Cell Reference Method. *Minerals Engineering*. 178 (15). https://doi.org/10.1016/j.mineng.2022.107411
[16] Eskanlou, A., Shahbazi, B., Vaziri Hassas, B. (2018). Estimation of flotation rate constant and collision efficiency using regression and artificial neural networks. *Separation Science and Technology*, 53 (2): 374-388. https://doi.org/10.1080/01496395.2017.1386216
[17] Hewitt, D., Fornasiero, D. & Ralston, J., (1995). Bubble–particle attachment. *Journal of the Chemical Society, Faraday Transactions*, 91(13): 1997-2001. https://doi.org/10.1039/FT9959101997
[18] Girgin, E. H., Do, S., Gomez, C. O. & Finch, J. A., (2006). Bubble size as a function of impeller 339 speed in a self-aeration laboratory flotation cell. *Minerals Engineering*, 19(2): 201-203. https://doi.org/10.1016/j.mineng.2005.09.002
[19] Jameson, G. J., Nam, S. & Young, M. M. (1977). Physical factors affecting recovery rates in flotation. *Mineral Science Engineering*, 9: 103-118.
[20] Schulze, H. J., (1989). Hydrodynamics of bubble-mineral particle collisions. *Mineral Processing and Extractive Metallurgy Review*, 5: 43-76. https://doi.org/10.1080/08827508908952644
[21] Rodrigues, R. T. & Rubio, J. (2003). New basis for measuring the size distribution of bubbles. *Minerals Engineering*, 16(8): 757-765. https://doi.org/10.1016/S0892-6875(03)00181-X
[22] Dukhin, S. S., Miller, R. & Loglio, G. (1998). Physico-chemical hydrodynamics of rising bubble. *Studies in Interface Science*, 6: 367-432. https://doi.org/10.1016/S1383-7303(98)80025-2
[23] Bruce, H. Kim. (2003). Modeling of hindered-settling column separations. A PhD thesis in mineral processing, The Pennsylvania State University, 11-13.
[24] Hu, Y., Qiu, G. & Miller, J. D. (2003). Hydrodynamic interactions between particles in aggregation and flotation. *International Journal of Mineral Processing*, 70(1-4): 157- 170. https://doi.org/10.1016/S0301-7516(03)00023-1
[25] Koh, P. T. L. & Schwarz, M. P., (2006). CFD modelling of bubble-particle attachments in flotation cells. *Minerals Engineering*, 19(6-8): 619-626. https://doi.org/10.1016/j.mineng.2005.09.013
[26] Dai, Z., Fornasiero, D. & Ralston, J. (1999). Particle-bubble attachment in mineral flotation. *Journal of Colloid and Interface Science*, 217(1): 70-76. https://doi.org/10.1006/jcis.1999.6319
[27] Flint, L. R. & Howarth, W. J. (1971). The collision efficiency of small particles with spherical air bubbles. *Chemical Engineering Science*, 26 (8): 1155-1168. https://doi.org/10.1016/0009-2509(71)87002-1
[28] Yoon, R. H. (2000). The role of hydrodynamic and surface forces in bubble-particle interaction. *International Journal of Mineral Processing*, 58 (1-4): 129-143. https://doi.org/10.1016/S0301-7516(99)00071-X
[29] Nguyen, A. V., Ralston, J. & Schulze, H. J. (1998). On modeling of bubble–particle attachment probability in flotation. *International Journal of Mineral Processing*, 53(4): 225-249. https://doi.org/10.1016/S0301-7516(97)00073-2
[30] Bloom, F. & Heindel, T. J. (2003). Modeling flotation separation in a semi batch process. *Chemical Engineering Science*, 58(2): 353-365. https://doi.org/10.1016/S0009-2509(02)00525-0
[31] Mika, T. S. & Fuerstenau, D. W. (1968). A microscopic model of the flotation process. Eighth International Journal Miner Process congress, Leningrad, 246.